Practical Thermal Model for a Radiant Tubes Annealing Furnace

Angel García-Martino*, María Manuela Prieto

Angel García-Martino
ArcelorMittal R&D Technological Centre, Avilés 33400, Asturias, Spain
E-mail: angel.garcia-martino@arcelormittal.com

María Manuela Prieto
Department of Energy, University of Oviedo, Campus de Viesques, Gijón 33204, Asturias, Spain

Abstract

Modeling of vertical radiant tube annealing furnaces has proven to be one of the best tools to improve the performance of a galvanizing line. However, there is a lack of a practical model able to consider the temperature and status of the radiant tubes, which are key elements in the capacity of the furnace. The model proposed divides the furnace in several segments and compares the radiated heat, that is exchanged between the radiant tubes and the strip, and the heat required to increase the temperature of the mass flow on the strip. This comparison is represented as an implicit equation where the strip‘s temperature is obtained by iteration. The model is validated calculating the final temperature of more than five hundred coils divided in four different steel families. The 90% of the calculated temperatures are within a 2% deviation range compared to the measured temperatures. This model combines good accuracy in the results with low computational times, allowing the simulation of hundreds of coils in a few minutes.

Keywords: annealing, furnace model, radiant tubes

1. Introduction

Galvanizing lines can process a wide range of strip formats from different steel families, each one with its own thermal cycle requirements. Each combination of these parameters will determine a maximum line speed, which is limited by the furnace capacity. For thinner strips, the furnace can achieve the required annealing temperature without overheating the radiant tubes, but when the entry thickness is higher than the *critical thickness*, the heating capacity of the furnace is the limiting factor. The higher the target temperature of the strip is, the lower the *critical thickness*. Due to the mentioned facts, characterization of annealing furnaces is vital in determining the maximum performance of a galvanizing line.

The capacity of a radiant tube furnace is given by its number of radiant tubes and type of burners. Depending on the type of burners, the efficiency of the combustion varies from 55 to 75% [1]. Most of the energy radiated by the tube is absorbed by the strip, but another part is lost across the furnace insulation, removed by the cooling systems of pyrometers and other elements within the furnace and employed to heat the furnace atmosphere[2].

The furnace capacity is affected by leaks or cracks on the surface of the tubes. Depending on the size of the leak, it could cause various effects ranging from strip pollution due to combustion byproducts to a total collapse of the radiant tube. For this reason, when a crack is detected, it is necessary to close the tube resulting in the furnace losing of heating capacity. The causes of cracks in the radiant tubes are several and interrelated [3], and the study of the root causes of radiant tube failure have been addressed several times in the literature [4-6]. Some of them are inherent to the material or the process requirements and cannot be avoided, but their combined effect can be mitigated acting over certain process parameters. Failure can be prevented by modifying the design or materials of the tube to improve its resistance to deformation [4] or acting over the maximum working temperature of the radiant tubes [5]. Therefore, many of the radiant tubes of the furnace are normally provided with a thermocouple placed at their hottest point, to control the evolution of the temperature and to avoid going past the tube's safe working limit.

Modeling of annealing furnaces is one of the best tools to improve the performance of a galvanizing line. There are several references in the literature about furnace models: some of them require the use of FEM, which entails an increase in complexity and longer computational time in case of 3D [6], but can be simplified to 2D and used online [7] ; others ,based on neural networks [8,9], are used to monitor the performance of the furnace over time; and finally, there are some models including combustion [10,11] that fulfill control purposes with a certain degree of accuracy. There are some other examples of modelling of the complete furnace system, including the furnace rolls and the combustion process [6, 12-15], however, none of these different approaches use the radiant tube temperatures or the status of the radiant tubes as is proposed in the model presented in this paper.

2. Case study and objectives

Arcelormittal Galvanizing Line Avilés 2 (Spain) is a line oriented to automotive market products. The line has a vertical radiant tube furnace divided in six sections: preheating, heating, soaking, slow cooling, rapid cooling and overaging (Fig. 1). The heating and soaking sections are provided with W shaped radiant tubes to heat up the strip by combustion of natural gas. The line used to suffer an atypically high rate of radiant tube collapses per year (over 25 % of the total), which was seriously affecting its productivity.

The mathematical model that controls the line sets a given thermal profile to the different zones of the furnace depending on the speed, thickness and required target temperature. This thermal profile implies differences in temperature between the different heating zones, which are referred to as *steps.*

Table 1 may be interpreted as follows: for the process conditions (target temperature and strip format), the actual temperatures in zones 1 to 8 must be within the range given respecting the reference taken at furnace end (zones 9 and 10).

This model works using zone temperature, with the temperature of the tubes being only a limitation that will switch off the zone in case the tubes work over their temperature limit over a period of time. This condition is continuously checked by thermocouples installed in two tubes per zone. If the temperature of any of these thermocouples stays over the safe limit during a certain time, the control limits the injection of gas until the temperature of the tubes decreases.

To reduce the number of breakages of radiant tubes and minimize the impact on the productivity, it is necessary to change the furnace's thermal profile in order to reduce the peak temperature of the tubes, while keeping the global heating capacity constant. To accomplish this objective, it is necessary to perform simulations of the furnace thermal performance to study different heating strategies, avoiding the cost of actual line trials that, in addition, could cause rejections of the processed material. This situation led to the development of a new offline heating model.

The new model must allow the calculation of the strip temperature profile based on the temperatures of the radiant tubes, instead of the zone temperatures, to avoid the overheating of the radiant tube which was identified as one of the root causes of tube failure. Also, it should be easy to change the number of available radiant tubes for the calculations and this way assessing the actual capacity of the line. In addition, it should be able to simulate different scenarios and select the critical locations of the furnace where the replacement of a radiant tube is required, as due to with the cost cutting affecting the maintenance budget it is necessary to minimize the number of radiant tubes replaced and identify the ones in critical condition. Lastly, the model might be used to study the furnace bottleneck through the simulation of different furnace conditions.

3. Methodology

3.1 Model description

The key concept used in the development of this model was to use as input the data available to the line operator at any moment. Another basic principle was the intention of keeping the physical basis as simple as possible with the purpose of limiting calculation time and enabling the evaluation of hundreds of cases in a very short time.

The first step was the analysis of the key parameters needed to calculate the strip's temperature: strip's format, speed, type of steel and zone temperatures were identified as the main ones. Afterwards, the physical modelling was addressed assuming the following simplification: as the predominant heat exchange mechanism in the furnace is radiation [10,16,17] the model calculates the temperature of the strip based only on the temperature of the radiant tubes. This hypothesis limits the model capabilities, which can only study the furnace in steady conditions, but this is still aligned with the model requirements.

The specific heat of steel is often used as a fixed value; this is valid for small temperature changes but modelling the annealing process requires calculating temperature changes of hundreds of degrees, so this approximation is no longer valid.

It was necessary to characterize the geometry of Avilés 2 furnace. In a vertical furnace with radiant tubes, the strip is driven between the radiant tubes across the furnace passing around the rolls located at the top and the bottom of the furnace. In the path between two consecutive rolls, the strip moves across two furnace control zones. Each furnace zone is composed of a series of radiant tubes managed by the same control loop. The Avilés 2 furnace has twelve zones, eight in the heating and four in the soaking.

The minimum strip length used for the calculations has been named as *segment* (Fig. 2). Each segment represents the length of strip that moves between the radiant tubes belonging to the same zone. Between each two consecutive rolls, the strip moves through two segments.

The length of a segment S_i is calculated on the base of the number of radiant tubes available in the i-th section, (Fig. 2c). The model can be easily adapted to a radiant tube failure situation by reducing this length S_i at the corresponding furnace section.

Each segment uses the temperatures of the thermocouples placed in the selected radiant tubes per zone as an input for the calculation, this way it is guaranteed that the tubes will be working in the safe area.

The proposal of a 2-D model in Equation (1) simplifies the standard approach, and instead of calculating the view factor in enclosures [18], the geometry consisting in infinite plane and row of cylinders is used [20] in Equation (2), being d and D the distances (Fig. 2d), A_{yz} the area and σ the Bolzman constant.

$$P_{T-S} = \sigma A_{yz} F_1 (T_{Tubes}^4 - T_{Strip}^4) \tag{1}$$

$$F_1 = 1 - \left[1 - \left(\frac{D}{d}\right)^2\right]^{\frac{1}{2}} + \left(\frac{D}{d}\right) tan^{-1}\left[\left(\frac{d^2 - D^2}{D^2}\right)^{1/2}\right] \tag{2}$$

P_{strip} in Equation (3) is the power required to increase the temperature of the mass flow, being v the strip speed, A_{xy} the strip section, ρ the density and $C_e\ (T)$ the specific heat.

$$P_{strip} = v A_{xy} \rho C_e(T) dT_{strip} \tag{3}$$

Areas in Equation (1) and (2) are in different planes: A_{yz} represents the length of the tubes in the y-axis (B) and the strip movement in the z-axis, meanwhile in the strip section A_{xy} the x-axis is the strip thickness (e) and the y-axis corresponds to the strip width (b).

Taking differentials in Equation (1) and Equation (3), the heat transfer in both sides of the strip is represented in Equation (4):

$$2B\varepsilon\sigma F_1 \left(T_{Tubes}^4 - T_{Strip}^4\right) dz = v e b \rho C_e(T) dT \tag{4}$$

A piecewise polynomial approximation is used for describing $C_e(T)$. The integration of Equation (4) using this polynomial is too complex, so in a first step $C_e(T)$ is taken as constant to obtain the expression in Equation (5), that corresponds to an implicit equation where strip temperature is obtained by iteration. The correction factor *k* is introduced to be used later during the model adjustment to adjust the difference between calculated and observed temperatures.

$$Z_i^* = \frac{kveb\rho C_e(T_i)}{8B\varepsilon\sigma F_1 T_{Tubes_i}^3}\left(2\mathrm{atan}\frac{T_i}{T_{tubes_i}} + \ln\frac{T_{tubes_i}+T_i}{T_{tubes_i}-T_i} - 2\mathrm{atan}\frac{T_{i-1}}{T_{tubes_i}} - \ln\frac{T_{tubes_i}+T_{i-1}}{T_{tubes_i}-T_{i-1}}\right) \quad (5)$$

This equation is solved by iteration (Fig. 3) along the 38 segments in which the furnace is divided. The final value of T_i is calculated by iteration, ending when the difference between calculated lenght (Z_i^*) and real lenght (S_i) of the segment *i* is lower than a given value (0.1). The values of T_i^* are calculated using Regula-Falsi method, within a range given by the temperature at the previous segment (T_{i-1}) and T_{i-1} plus an increment proportional to the target temperature at the end of the furnace. During the iterations the value of $C_e(T)$ is calculated using the estimated temperature T_i^*. The global iteration ends when the error at the exit pyrometer is less than 2º C.

3.2 Model tuning

The source of data for the elaboration of the model was the line database which stores the process data and the $C_e(T)$ curves of the different steel families. The emissivity depends on the temperature and strip's surface conditions [18], but as there is no curve representing its evolution, the set value in the pyrometers (0.3) is used. During model's tuning process, a slight adjustment may be performed.

The entry parameters of the model are: strip format, type of steel, initial temperature and speed or strip target temperature. If the maximum speed for a target temperature is requested, the outputs of the model are the speed, the strip thermal profile and the temperature of the tubes in each zone. If both, speed and target temperature of the strip are given, the outputs will be the thermal profile of the strip and the temperature of the tubes in each zone. By changing the temperatures of the radiant tubes, it is possible to study the furnace bottlenecks through the simulation of different furnace conditions, in some cases reaching a potential higher process speed than the calculated by the provider

The process values required are mean coil values, so it was necessary to make a previous filtering to remove outliers. From the final data set, the ranges of temperature of the tubes in each zone for each steel family are defined (Fig. 4 left). These values, in combination with the zone *steps* are used to limit the range of feasible temperatures of the tubes and therefore reducing the time required in the model for the calculation.

The adjustment factor k and the temperature of radiant tubes are calculated in two iterations. The aim of the first one is to define the specific range of temperatures for each format and an initial value of k. The k is adjusted to minimize the difference between real and calculated temperatures of the radiant tubes. Its value is 0.85 for most of steels, but for a few of them it is slightly lower (0.75). The maximum and minimum values of the temperature of the radiant tubes calculated for each zone and format will set the new limits (Fig. 4 right) used in the second iteration, where the temperatures of the tubes are recalculated using a fix k which is the mode of the values of k obtained during the first iteration. The accuracy of the simulation can be calculated comparing the real temperature with the calculated temperature as follows:

$$\varepsilon(\%) = \frac{T_{cal} - T_{real}}{T_{real}} 100 \qquad (6)$$

4. Testing of the model

The test data set was formed by 600 coils corresponding to ten days of line production. As the model is oriented to simulate steady conditions, and during the production some events can affect the speed as well as the final coil temperature, it was necessary to make a filtering of the set of coils attending to stability criterion. The average speed, radiant tube and strip temperature per coil were calculated using the time-based process signals, and the cases which did not fulfill the following conditions were discarded: (1) standard deviation of the speed less than 2, and (2) standard deviation of the coil temperature at the exit lower than 20. After the filtering was performed, the remaining 569 coils were classified by steel families in four groups, as shown in **Table 2**: Interstitial Free (IF, 200 coils), Low Carbon (LC, 216 coils), High Strength Low Alloy (HSLA, 125 coils) and Dual Phase (DP, 28 coils).

Five different control points were established to evaluate the global accuracy of the model: two at pyrometers P2 and P3 (Fig. 1) to evaluate the accuracy of the strip temperature calculations, and three at zones 1-2, 5-6 and 9-10 to evaluate the accuracy of the temperatures calculated for the radiant tubes. In the case of the radiant tubes, the T_{real} is, in each case, the average of temperatures of four tubes provided with thermocouples.

The charts (Fig 5) show the results of the simulation for the different steel families studied: a) and b) corresponds to IF, c) and d) to low carbon, e) and f) to HSLA and g) and h) to Dual Phase. The size of the bars represents the number of cases classified by the temperature error percentage, which is calculated as described in equation 6.

It is observed that better accuracy is obtained in the case of g and h. This is explained due to two factors: the curve describing the specific heat is available and most of the formats simulated are over the *critical thickness* limits, therefore, the adjustment factor *k* is calculated for a group of coils which speed is directly limited by the heating capacity. In the other families, despite that the general results are good, the accuracy is lower than in the case of the Dual Phase for the same reasons, or the specific heat curve corresponding to this family (as in the case of Low Carbon) is not available or the percentage of the coils below the corresponding *critical thickness* is too high which affects the calculation of the adjustment factor *k* (case of IF where half of the coils are below this limit). So, it can be concluded that the model is more accurate in the case of thicker formats than thinner ones and that it is required to have the steel characterized. Additional improvements in the accuracy of the calculations are expected if the convection mechanism is included.

Despite this limitation, it is still completely valid to study the furnace bottlenecks, when the power demand on the furnace can push the radiant tubes to work at temperatures that are too high.

The model is also used to optimize the replacement of broken radiant tubes when, due to time or budget constrictions, is not possible to replace all of them. The graph (Fig. 6) shows the effect on the nominal speed of the position of the broken radiant tubes: cases A and C correspond respectively to a failure of the 5% and 10% of the tubes homogeneously distributed in the furnace, and in the cases B and D the 5% and 10% of failures are distributed only among zones 5 to 8 of the furnace.

5. Conclusions

A mathematical model of an indirect fired furnace was derived. The objective of this research was to obtain a model that could be used by the production line team as a simulation tool using the production data as input, with the flexibility to be adapted to real furnace conditions and considering the limitation on radiant tube temperatures needed to minimize the maintenance as long as possible. This objective was successfully fulfilled, leading to a noticeable increase in line productivity and maintenance savings.

The main advantage of this model with respect to previous models is that it considers the temperature of the radiant tubes to prevent overheating problems that could lead to tube failure. As mentioned throughout the text, the model combines good accuracy in the calculations with low computational times, allowing the simulation of hundreds of coils in just a few minutes and it can be easily adapted to the current conditions of the furnace. It also has an application to maintenance works, prioritizing the replacement of damaged tubes as function of its effect on the capacity of the furnace.

Acknowledgements

The authors greatfully acknowledge ArcelorMittal for supporting this investigation and the Avilés 2 staff for their collaboration during the development of trials.

References

[1] J.G. Wuenning, "Regenerative burners for heat treating furnaces" in 8th European conference on industrial furnaces and boilers (INFUB) 25, (2008) 28.

[2] W. Trinks, M. H, Mawhinney, R. A. Shannon, J. R. Garvey, R. J. Reed, Industrial furnaces, Wiley, Hoboken, (2004) 185–193.

[3] M. A. Irfan, W. Chapman, "Thermal stresses in radiant tubes due to axial, circumferential and radial temperature distributions" Appl. Therm. Eng. 29, (2009) 1913-1920.

[4] N. Schmitz, M. Hellenkamp, H. Pfeifer, E. Cresci, J. Wünning, M. Schönfelder, "Radiant Tube Life Improvement for Vertical Galvanizing Lines" presented at the 10th International Conference on Zinc and Zinc Alloy Coated Steel, Toronto, (2015)

[5] A. Ul-Hamid, H. M. Tawancy, A. R. I. Mohammed, N. M. Abbas, "Failure analysis of furnace radiant tubes exposed to excessive temperature" Eng. Fail. Anal. 13, (2006) 1005-1021.

[6] Z. W. Kang, T. C. Chen, "Three-dimensional temperature distributions of strip in continuous annealing line" Appl. Therm. Eng. 58, (2013) 241-251.

[7] N. Depree, J. Sneyd, S. Taylor, M.P. Taylor, J.J.J. Chen, S. Wang, M. O`Connor, "Development and validation of models for annealing furnace control from heat transfer fundamentals" Comp. and Chem. Eng. 34, (2010) 1849-1853.

[8] A. Pernía-Espinoza, M. Castejón-Limas, A. González-Marcos, V. Lobato-Rubio, "Steel annealing furnace robust neural network model" Ironmak. Steelmak. 32, (2005) 418-426.

[9] S. Li, Q. Chen, G. B. Huang, "Dynamic temperature modeling of continuous annealing furnace using GGAP-RBF neural network" Neurocomputing 69, (2006) 523-536.

[10] M. Niederer, S. Strommer, A. Steinboeck, A. Kugi, "A simple control-oriented model of an indirect-fired strip annealing furnace" Int. J. Heat Mass Transf. 78, (2014) 557-570.

[11] Y. C. Tian, C.-H. Hou, F. Gao, "Mathematical Model of a Continuous Galvanizing Annealing Furnace" Dev. Chem. Eng. Miner. Process. 8, (2000) 359-374.

[12] M. M. Prieto, F. J. Fernández, J. L. Rendueles, "Development of stepwise thermal model for annealing line heating furnace" Ironmak. Steelmak. 32, (2005) 165-170.

[13] T. C. Chen, C. H. Ho, J. C. Lin, L.W. Wu, "3-D temperature and stress distributions of strip in preheating furnace of continuous annealing line" Appl. Therm. Eng. 30, (2010) 1047-1057.

[14] S. R. Carvalho, T. H. Ong, G. Guimarães, "A mathematical and computational model of furnaces for continuous steel strip processing" J. Mater. Process. Technol. 178, (2006) 379-387.

[15] H. Wu, R. Speets, F. Heeremans, O. Ben Driss, R. van Buren, "Nonlinear model predictive control of throughput and strip temperature for continuous annealing line", Ironmaking & Steelmaking 42, (2015) 570-578.

[16] S. Zareba, A. Wolff, M. Jelali, "Mathematical modelling and parameter identification of a stainless steel annealing furnace", Simul. Model. Prac. Th. 60, (2016) 15-39.

[17] M. McGuinness, S. Taylor, "Strip temperature in a metal coating line annealing furnace", Technical report, Mathematics in Industry (2004) http://www.math.auckland.ac.nz/deptdb/dept_reports/532.pdf.

[18] C. D. Wen, "Investigation of steel emissivity behaviors: Examination of Multispectral Radiation Thermometry (MRT) emissivity models" Int. J. Heat Mass Transf. 53, (2010) 2035-2043.

[19] F. Wan, Y. Wang, S. Qin, "Modeling of Strip Heating Process in Vertical Continuous Annealing Furnace" J. of Iron and Steel Research, Int. 19, (2012) 29-36.

[20] F. Incropera, D. P. Dewitt, T. L. Bergman, A. S. Lavine, Fundamentals of Heat and Mass Transfer, Hoboken, Wiley, USA (2007) 816.

Figure 1. Layout of Avilés #2 furnace

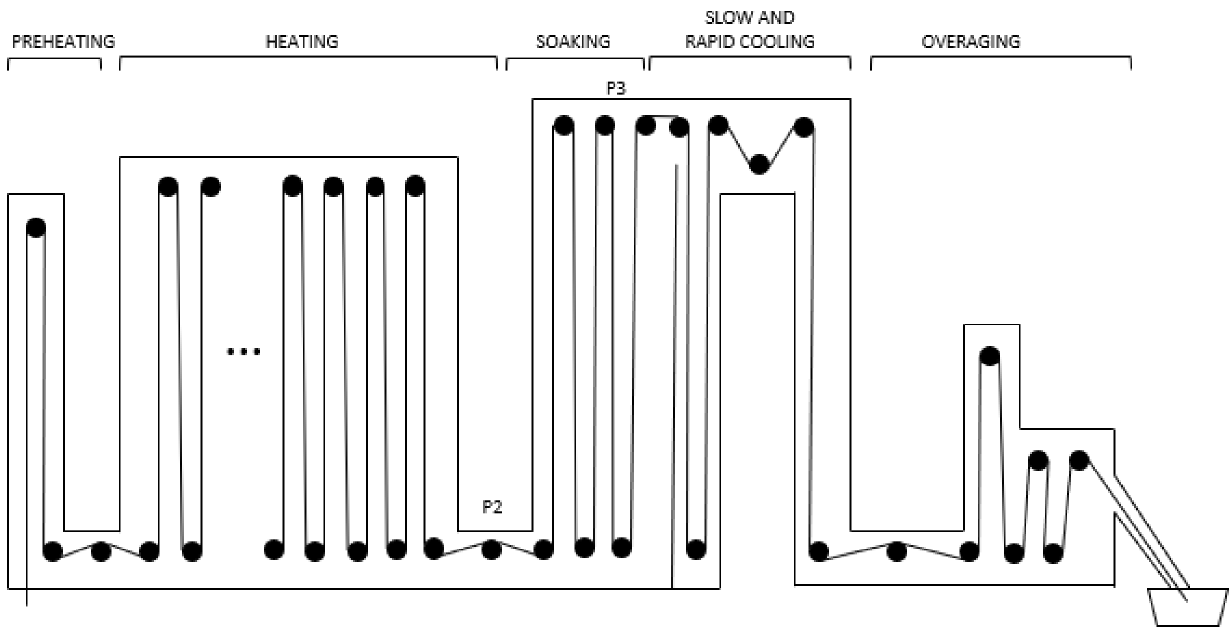

Figure 2. Strip (red line) passes between the radiant tubes, represented as squares (a). Each tube has four circular legs as shown in (b), constituting the radiation surface. The model calculates the heat exchange within dotted area represented in (c), which is defined as the segment

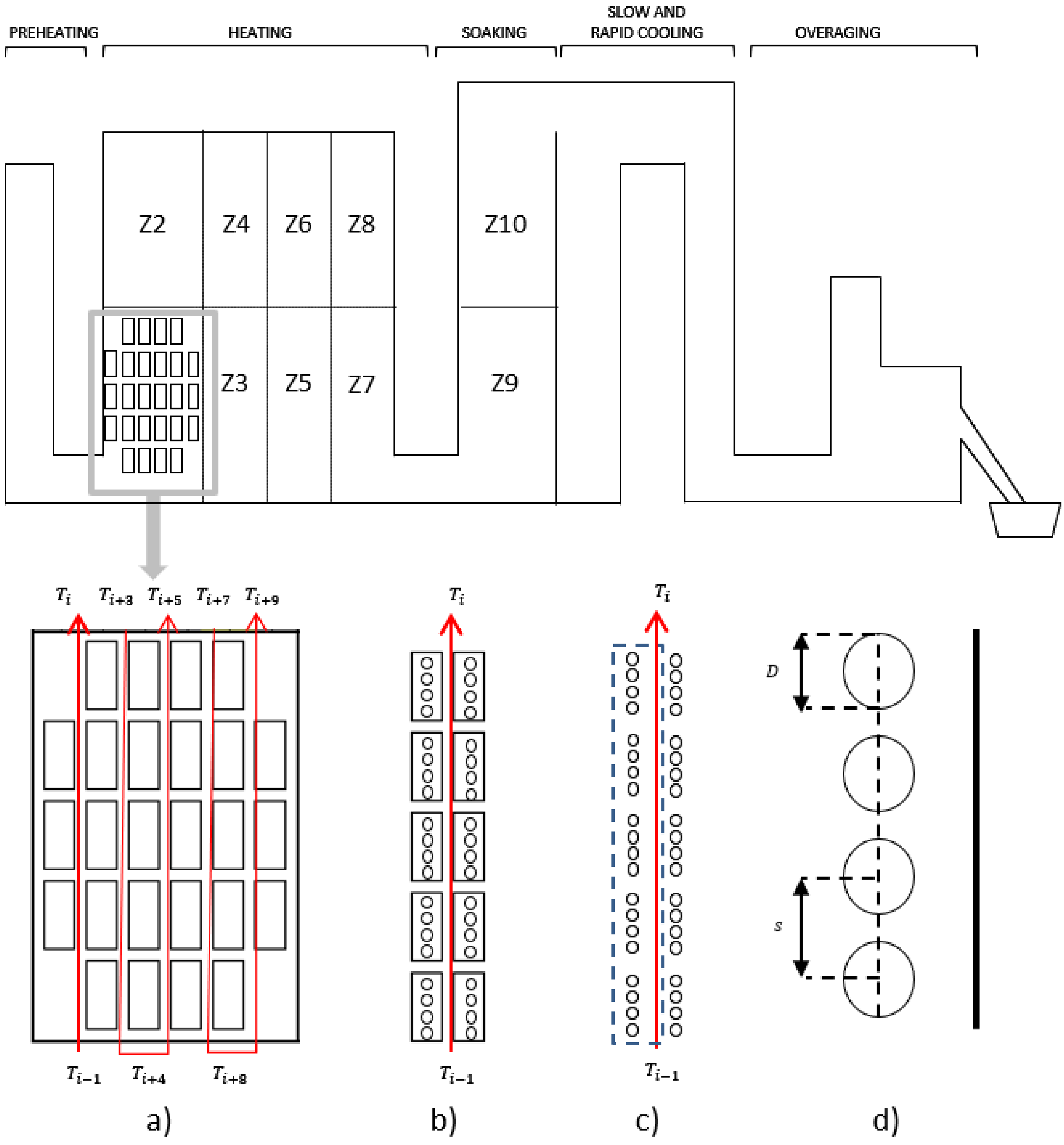

Figure 3. Calculation algorithm

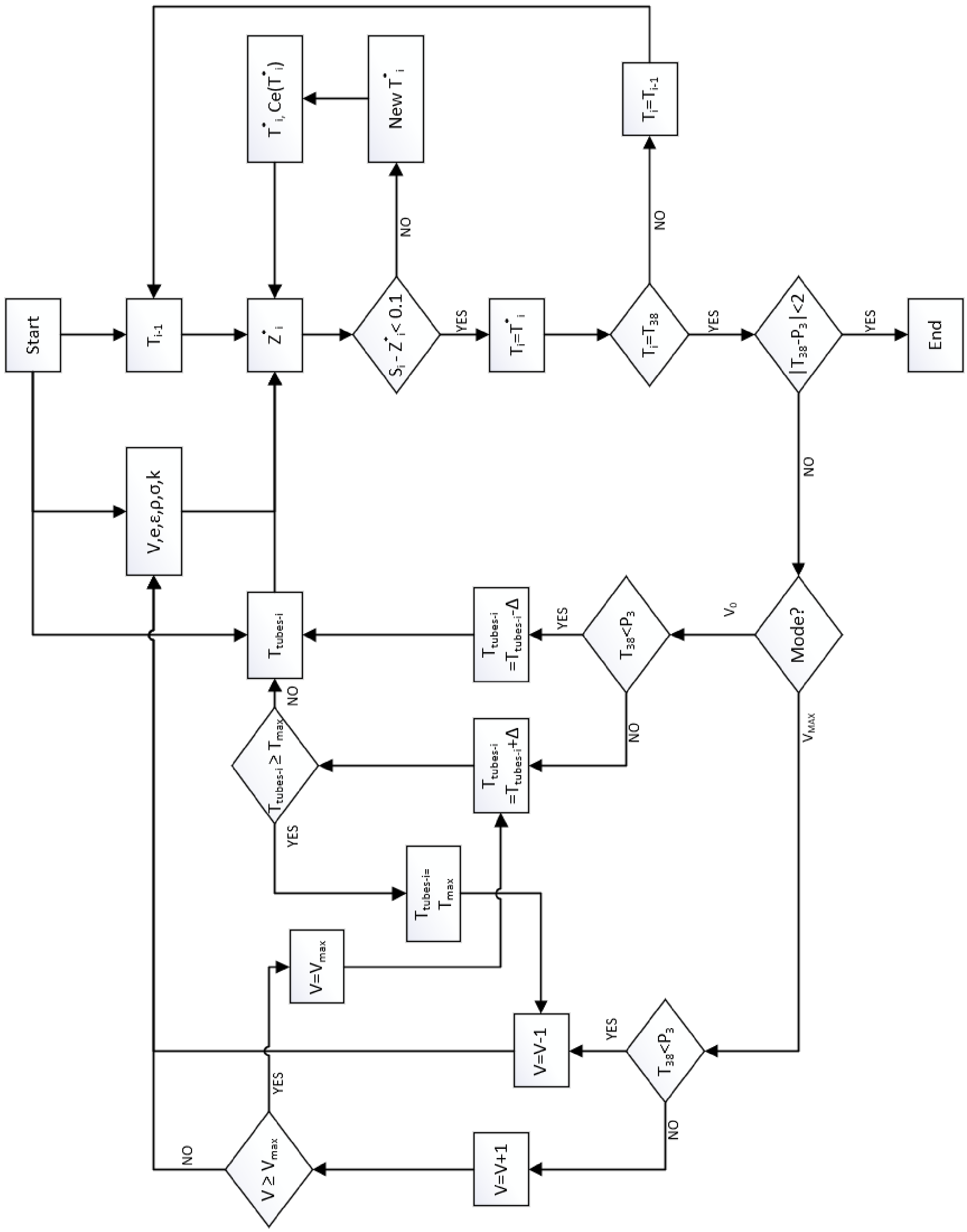

Figure 4. Initial temperature ranges for all strip formats are represented by lines, calculated temperature ranges for limited strip's formats are represented by rectangles (in white for formats and in black for temperatures)

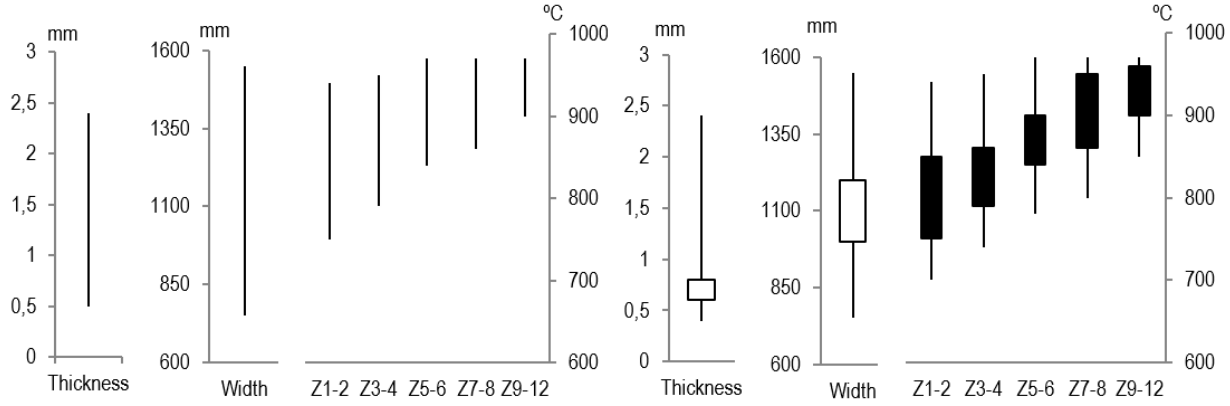

Figure 5. Simulations result. Temperature errors calculated as described in equation 6

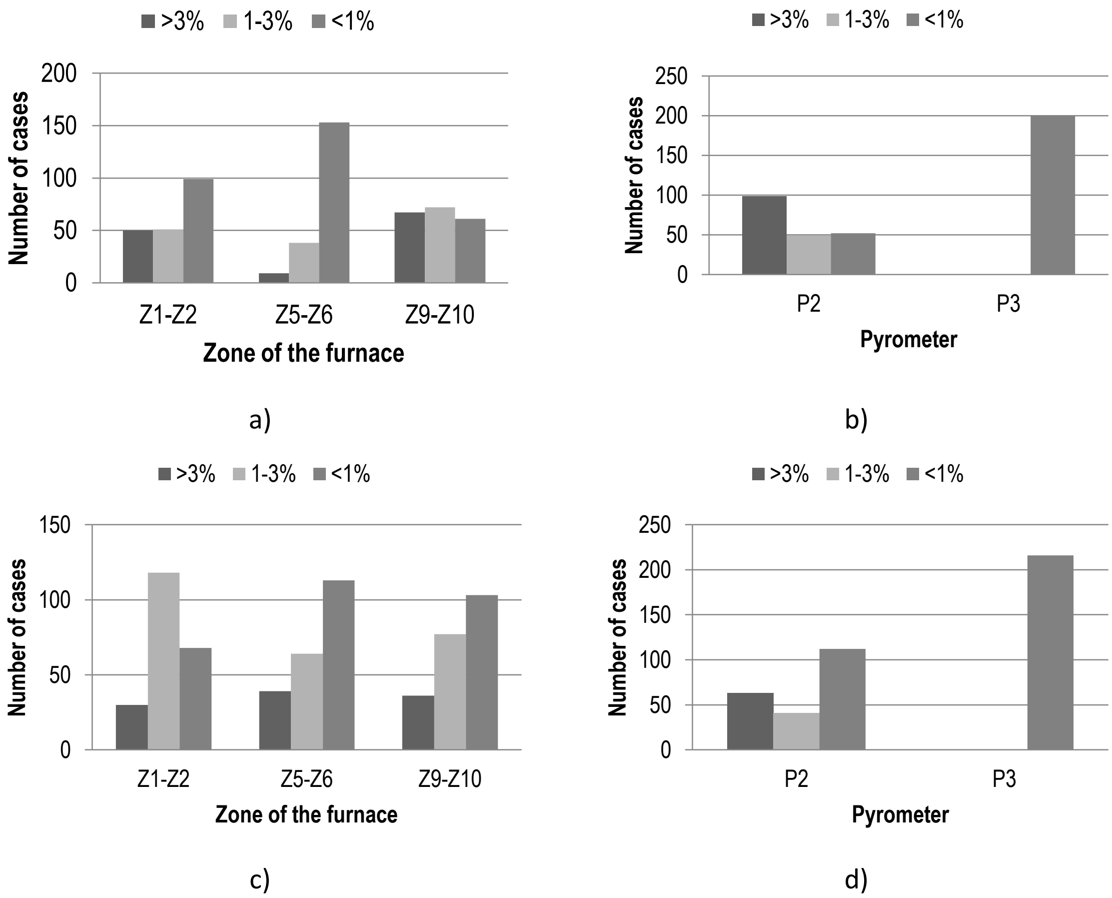

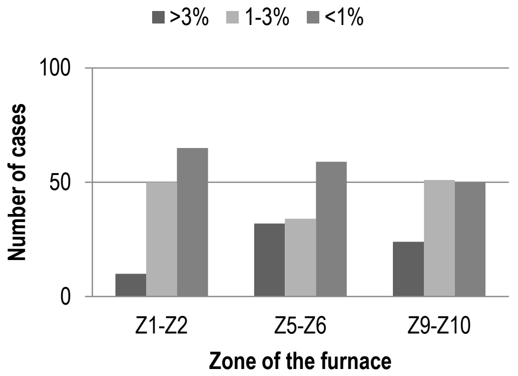

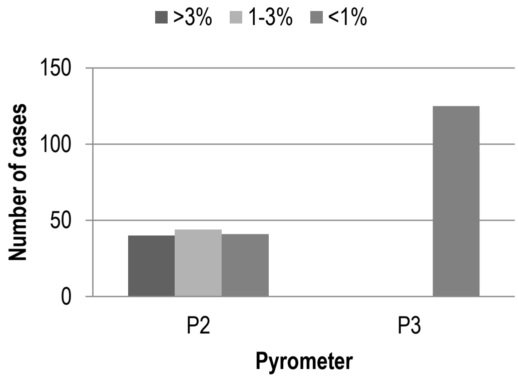

e)

f)

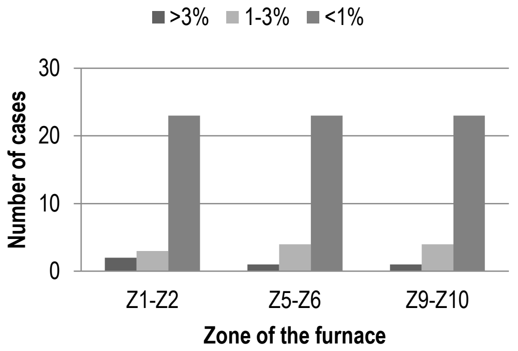

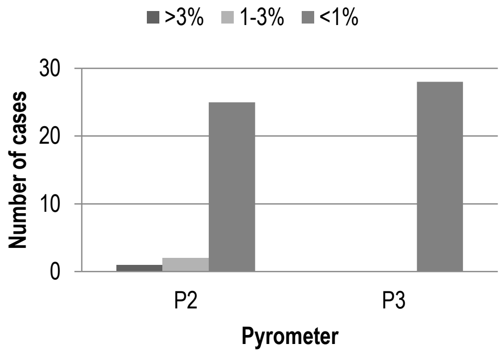

g)

h)

Figure 6. Effect of the position of damaged radiant tubes on line speed

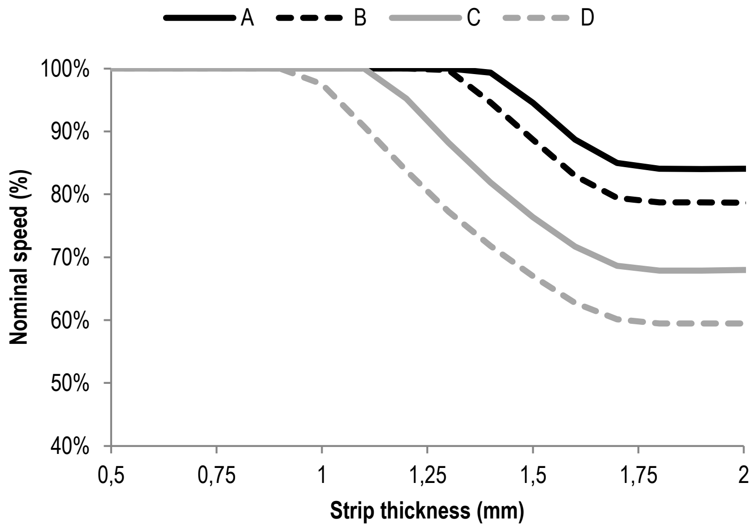

Table 1. Example of furnace steps

Target temp (ºC)		Thickness (mm)		Width (mm)		Zones 1 - 2 (ºC)		Zones 3 - 4 (ºC)		Zones 5 - 6 (ºC)		Zones 7 - 8 (ºC)	
780[1)]	820[2)]	0.6[1)]	0.8[2)]	1200[1)]	1349[2)]	-150[1)]	-100[2)]	-125[1)]	-50[2)]	-70[1)]	-20[2)]	-30[1)]	-10[2)]

780[1]	820[2]	0.9[1]	1.3[2]	1200[1]	1349[2]	-65[1]	-30[2]	-40[1]	-20[2]	-20[1]	0[2]	0[1]	0[2]
780[1]	820[2]	1.8[1]	2[2]	1200[1]	1349[2]	-30[1]	-15[2]	-30[1]	-10[2]	-10[1]	5[2]	0[1]	5[2]

[1] Minimum value; [2] Maximum value

Table 2. Steel families and process parameters ranges

Steel family	Steel grade	Number of coils	Thickness (mm)		Speed (mpm)		Target temp. (ºC)	
IF	B100	97	0.5[1]	2[2]	40[1]	160[2]	750[1]	800[2]
	B102	52	0.5[1]	2[2]	40[1]	160[2]	725[1]	775[2]
	B105	51	0.5[1]	2[2]	60[1]	160[2]	730[1]	800[2]
Low carbon	B012	110	0.5[1]	2[2]	40[1]	160[2]	750[1]	790[2]
	B048	54	0.5[1]	2[2]	60[1]	160[2]	725[1]	825[2]
	B085	52	0.5[1]	2[2]	40[1]	160[2]	750[1]	825[2]
HSLA	D071	125	0.7[1]	2[2]	40[1]	160[2]	750[1]	830[2]
Dual Phase	D09X	28	0.9[1]	2[2]	60[1]	160[2]	775[1]	850[2]

[1] Lower limit; [2] Upper limit